Implementation and Adjustment of CPML for CE-FDTD Algorithm

Bojana Nikolic, Bojan Dimitrijevic, Slavoljub Aleksic, Nebojsa Raicevic, Zorica Nikolic

University of Nis, Faculty of Electronic Engineering, Nis, Serbia, bojana.nikolic@elfak.ni.ac.rs, bojan.dimitrijevic@elfak.ni.ac.rs, slavoljub.aleksic@elfak.ni.ac.rs, nebojsa.raicevic@elfak.ni.ac.rs, zorica.nikolic@elfak.ni.ac.rs

Abstract— **A complex-envelope finite difference time domain (CE-FDTD) algorithm has been proposed in the literature as one of FDTD formulations that is very general. However, this method, didn't receive a lot of scientific attention, since the introduced complexity wasn't quite justified by the obtained gain in maximum time step size. Nevertheless, there is still a strong motivation to study this formulation, since it can potentially be, in combination with high order accuracy FDTD approaches, a significant tool to combat the accuracy deterioration due to numerical dispersion. A method of choice for termination of CE-FDTD computational domain was the convolutional perfectly matched layer (CPML), since it is considered to be superior over other commonly used techniques. Yet, the application of CPML in CE-FDTD environment isn't straightforward. In this paper a modification of conventional CPML is performed in order to be used for termination of CE-FDTD computational domain. The modified CPML, along with CE-FDTD algorithm has been implemented in an own developed simulation environment and tested through various simulation cases. The functionality of the proposed CPML is illustrated on the example of a dipole antenna. The observed behavior of the boundary region fully corresponds to the propagation through the free space, without any undesirable reflections.**

I. Introduction

The finite difference time domain (FDTD) method is a full wave time domain differential equation based technique that received huge attention in the literature recently. It is a versatile method that was proposed by Yee [1] for two dimensional problems with metal boundaries. Nowadays the FDTD method is one of the most popular methods for simulation and analysis of electromagnetic problems, ranging from antennas, microwave wave circuits, electromagnetic scattering to bioelectromagnetics and nanophotonics [2], [3]. However, the conventional FDTD formulation shows low computational efficiency when applied to the bandpass-limited (narrow band) signals that are very common in communication systems. Namely, in order to keep the numerical dispersion low, a time step has to be small (with the respect to the highest frequency in the signal), although useful envelope information occupies only a small bandwidth around the high carrier frequency [4].

In order to overcome this problem, a complex-envelope FDTD (CE-FDTD) scheme has been proposed [5]. Using this method, the signal can be sampled in accordance with the bandwidth of the signal rather than its maximum frequency, which yields the time step significantly increased in comparison with the conventional FDTD. A comprehensive stability and numerical dispersion analysis of CE-FDTD can be found in [4]. It is, though, shown that the gain in maximum allowed time step isn't enough to make the CE-FDTD formulation favourable in terms of computation efficiency when comparing to the conventional FDTD. In particular, maximal time step allowed for stabile and practically usable CE-FDTD results is very much dependant on the relative sizes of carrier wavelength and spatial steps [4]. However, it is still important to study this formulation, since it can potentially be, in combination with high order accuracy FDTD approaches, a significant tool to combat the accuracy deterioration due to numerical dispersion.

The perfectly matched layer (PML) absorbing medium [6] is considered to be the most robust and efficient technique for the termination of FDTD computational domain [7]. One particular PML implementation, referred to as the convolutional PML (CPML) seems to outperform the other implementations of the PML, offering a number of advantages [8]. CPML is based on the stretched coordinate form [9] and the use of complex frequency shift (CFS) of PML parameters [10]. It is shown that the CFS-PML is highly absorptive of evanescent modes and can provide significant memory savings when computing the wave interaction of elongated structures, sharp corners, or low frequency excitations [8]. However, it can't be directly applied to the CE-FDTD algorithm.

In this paper a modification of conventional CPML is performed in order to support termination of CE-FDTD computational domain. The modified CPML, along with CE-FDTD algorithm has been implemented in an own developed simulation environment and tested through various simulation cases. The functionality of the proposed CPML is illustrated on the example of a dipole antenna.

II. CE-FDTD Formulation

A detailed description of CE-FDTD algorithm can be found in [4], [5]. A narrow band signal can be presented as

$$\left(H_{pv}, E_{pv}\right) = \mathrm{Re}\left\{\left(\hat{H}_{\nu}, \hat{E}_{\nu}\right) e^{j\omega_c t}\right\}, \nu = x, y, z\,, \qquad (1)$$

where ω_c is the carrier frequency, $j = \sqrt{-1}$ is imaginary unit and operator $\mathrm{Re}\{\cdot\}$ returns the real part of a complex number. $\hat{H}_{\nu}$ and $\hat{E}_{\nu}$ denote associated complex-envelope representations

$$(\hat{H}_\nu, \hat{E}_\nu) = \left(\hat{H}_{p\nu}, \hat{E}_{p\nu}\right) + j\left(\hat{H}_{q\nu}, \hat{E}_{q\nu}\right),\ \nu = x, y, z \quad (2)$$

Magnitudes $\left(\hat{H}_{p\nu}, \hat{E}_{p\nu}\right)$ and $\left(\hat{H}_{q\nu}, \hat{E}_{q\nu}\right)$ are in-phase and quadrature parts of $\left(\hat{H}_\nu, \hat{E}_\nu\right)$.

Using (1), CE Maxwell's equations can be obtained as

$$\varepsilon_x \frac{\partial \hat{E}_x}{\partial t} + \hat{\sigma}_{ex}\hat{E}_x = \frac{\partial \hat{H}_z}{\partial y} - \frac{\partial \hat{H}_y}{\partial z} \quad (3)$$

$$\mu_x \frac{\partial \hat{H}_x}{\partial t} + \hat{\sigma}_{mx}\hat{H}_x = \frac{\partial \hat{E}_y}{\partial z} - \frac{\partial \hat{E}_z}{\partial y} \quad (4)$$

where it is $\hat{\sigma}_{ex} = \sigma_{ex} + j\omega_c$ and $\hat{\sigma}_{mx} = \sigma_{mx} + j\omega_c$. Electric and magnetic conductivity are denoted as σ_{ex} and σ_{mx}, respectively. It should be mentioned that the magnetic conductivity σ_{mx} is, strictly speaking, not physically realistic, but is often used to describe magnetic losses [11] and it will be included in this analysis. This term was labeled as σ_{mx} in order to maintain similar notation in Faraday's and Ampere's law. For the brevity only equations for $\hat{E}_x$ and $\hat{H}_x$ field components are presented.

Applying the same techniques for spatial and temporal discretization as in conventional FDTD formulation (second-order accurate two-point central difference technique and time-average time approximation), one can obtain CE-FDTD update equations. For $\hat{H}_x$ and $\hat{E}_x$ field components, it is

$$\begin{aligned}\hat{H}^{n+1/2}_{x(i,j+1/2,k+1/2)} &= a_{x,H}\hat{H}^{n-1/2}_{x(i,j+1/2,k+1/2)} + \\ &+ b_{x,H}\left(\hat{E}^{n}_{y(i,j+1,k+1)} - \hat{E}^{n}_{y(i,j+1,k)}\right)\Big/\Delta z - \\ &- b_{x,H}\left(\hat{E}^{n}_{z(i,j+1,k+1)} - \hat{E}^{n}_{z(i,j,k+1)}\right)\Big/\Delta y\end{aligned} \quad (5)$$

$$\begin{aligned}\hat{E}^{n+1}_{x(i+1,j,k)} &= a_{x,E}\hat{E}^{n}_{x(i+1,j,k)} + \\ &+ b_{x,E}\left(\hat{H}^{n+1/2}_{z(i+1/2,j+1/2,k)} - \hat{H}^{n+1/2}_{z(i+1/2,j-1/2,k)}\right)\Big/\Delta y - \\ &- b_{x,E}\left(\hat{H}^{n+1/2}_{y(i+1/2,j,k+1/2)} - \hat{H}^{n+1/2}_{y(i+1/2,j,k-1/2)}\right)\Big/\Delta z\end{aligned} \quad (6)$$

$$\hat{H}^{n}_{u} = \hat{H}^{n}_{u(i,j,k)} = \hat{H}_u\left(i\Delta x, j\Delta y, k\Delta z, n\Delta t\right) \quad (7)$$

$$\hat{E}^{n}_{u} = \hat{E}^{n}_{u(i,j,k)} = \hat{E}_u\left(i\Delta x, j\Delta y, k\Delta z, n\Delta t\right),\ u = x, y, z \quad (8)$$

where Δt is the time step, Δx, Δy and Δz are spatial steps along x, y and z axis, respectively.

Update coefficients $a_{v,E}$, $b_{v,E}$, $a_{v,H}$ and $b_{v,H}$ ($v = x, y, z$) are given in Table I.

Since the main intention in application of the presented CE-FDTD algorithm is to maintain very small size of the spatial discretization steps, the numerical stability criterion in that case can be described by the relation [4]

$$\begin{aligned}\Delta t \le \Delta t_{\max} &= \\ &= 1\Big/\left(c\sqrt{(1/\Delta x)^2 + (1/\Delta y)^2 + (1/\Delta z)^2 - (\omega_c/2c)^2}\right).\end{aligned} \quad (9)$$

It can be noticed that criterion (9) limits the size of a time step less severely than Courant-Frederick-Levy (CFL) condition (which characterizes the stability of conventional FDTD algorithm). For this reason, CFL can be also used in the case of CE-FDTD algorithm.

TABLE I.
UPDATE COEFFICIENTS CE-FDTD [12]

Update Coefficients	
$a_{v,H}$	$\dfrac{1-\hat{\sigma}_{mv}\Delta t/(2\mu_v)}{1+\hat{\sigma}_{mv}\Delta t/(2\mu_v)}$
$b_{v,H}$	$\dfrac{\Delta t/\mu_v}{1+\hat{\sigma}_{mv}\Delta t/(2\mu_v)}$
$a_{v,E}$	$\dfrac{1-\hat{\sigma}_{ev}\Delta t/(2\varepsilon_v)}{1+\hat{\sigma}_{ev}\Delta t/(2\varepsilon_v)}$
$b_{v,E}$	$\dfrac{\Delta t/\varepsilon_v}{1+\hat{\sigma}_{ev}\Delta t/(2\varepsilon_v)}$

III. CPML ALGORITHM

The CPML implementation, based on the conventional FDTD formulation, along with undertaken code optimizations, is described in detail in [13]. In this paper, in order to terminate a CE-FDTD computational domain, a modification of CPML algorithm will be introduced. In that case update equations for $\hat{H}_x$ and $\hat{E}_x$ field components have the form

$$\begin{aligned}\hat{H}^{n+1/2}_{x} &= \hat{H}^{n-1/2}_{x} + \frac{\Delta t}{\mu_x}\frac{\Delta \hat{E}^{n}_{y}}{\Delta z} - \frac{\Delta t}{\mu_x}\frac{\Delta \hat{E}^{n}_{z}}{\Delta y} + \\ &+ \left(\Psi^{n}_{Eyz} - \Psi^{n}_{Ezy}\right)e^{-j\omega_c n\Delta t} + \\ &+ \frac{1-k_z}{k_z}\frac{\Delta t}{\mu_x}\frac{\Delta \hat{E}^{n}_{y}}{\Delta z} - \frac{1-k_y}{k_y}\frac{\Delta t}{\mu_x}\frac{\Delta \hat{E}^{n}_{z}}{\Delta y}\end{aligned} \quad (10)$$

$$\begin{aligned}\hat{E}^{n+1}_{x} &= \hat{E}^{n}_{x} + \frac{\Delta t}{\varepsilon_x}\frac{\Delta \hat{H}^{n+1/2}_{z}}{\Delta y} - \frac{\Delta t}{\varepsilon_x}\frac{\Delta \hat{H}^{n+1/2}_{y}}{\Delta z} + \\ &+ \left(\Psi^{n+1/2}_{Hzy} - \Psi^{n+1/2}_{Hyz}\right)e^{-j\omega_c (n+1/2)\Delta t} + \\ &+ \frac{1-k_y}{k_y}\frac{\Delta t}{\varepsilon_x}\frac{\Delta \hat{H}^{n+1/2}_{z}}{\Delta y} - \frac{1-k_z}{k_z}\frac{\Delta t}{\varepsilon_x}\frac{\Delta \hat{H}^{n+1/2}_{y}}{\Delta z}\end{aligned} \quad (11)$$

where it is

$$\Psi^{n}_{Euv} = p_v\Psi^{n-1}_{Euv} + q_v\frac{\Delta t}{\mu}\frac{\Delta \hat{E}^{n}_{u}}{\Delta v}e^{j\omega_c n\Delta t} \quad (12)$$

$$\Psi_{Huv}^{n+1/2} = p_v \Psi_{Huv}^{n-1/2} + \\ + q_v \frac{\Delta t}{\varepsilon_v} \frac{\Delta \hat{H}_u^{n+1/2}}{\Delta v} e^{j\omega_c \left(n+\frac{1}{2}\right)\Delta t} \quad (13)$$

$$q_u = \frac{\sigma_u}{\sigma_u k_u + k_u^2 \alpha_u} \left(\exp\left(-\frac{\Delta t}{\varepsilon_0} \left(\frac{\sigma_u}{k_u} + \alpha_u \right) \right) - 1 \right) \quad (14)$$

$$p_u = \exp\left(-\frac{\Delta t}{\varepsilon_0} \left(\frac{\sigma_u}{k_u} + \alpha_u \right) \right), \; u, v \in \{x, y, z\}. \quad (15)$$

Parameters k_i, σ_i and α_i inside the CPML are graded

$$\alpha_i = (1 - \xi_i / D)^{m\alpha} \, \alpha_{\max}, \quad (16)$$

$$k_i = 1 + (\xi_i / D)^m (k_{\max} - 1), \quad (17)$$

$$\sigma_i = (\xi_i / D)^m \sigma_{\max}, \quad i = x, y, z, \quad (18)$$

where $\alpha_{\max}$ is the value on the air–PML interface and $k_{\max}$ and $\sigma_{\max}$ at the outer boundary. Current position in CPML is denoted by ξ_i and m_α and m are CPML parameters. The width of the PML is denoted by D.

A detailed procedure of derivation for update equations (10)-(13) are given in Appendix.

In (10) and (11) it can be noticed that first three sum members are equivalent to the update equations for x components of magnetic and electric field in free space ((5) and (6)), respectively. The E and H field components are thus first updated in the particular elementary cell using standard FDTD updates, regardless of whether it belongs to the computational domain or CPML region. The cell is next tested if it is in CPML region. If yes, the rest parts of (10) and (11) are simply added in within the corresponding PML regions. Since (H_u, E_u) field elements are needed in auxiliary loops Ψ_{Euv}^{n} and $\Psi_{Huv}^{n+1/2}$ ($u, v \in \{x, y, z\}$) and only $(\hat{H}_u, \hat{E}_u)$ are available, complex field components are shifted into the band of high frequencies multiplying by $e^{j\omega_c (n+1/2)\Delta t}$ and $e^{j\omega_c n \Delta t}$, respectively. In this way, modified CPML boundary will function like the one that terminates two independent real computational domains.

IV. Simulation Results and Discussion

The CE-FDTD algorithm with the modified CPML has been implemented as one of the operating modes available in actual realized FDTD simulation environment. Its performance is verified in various simulation cases. For the purpose of illustration, an example of a dipole antenna is presented here. Differential Gaussian pulse is used as an excitation signal. The number of used CPML layers is 8.

In Figs. 1-6 one can follow the propagation of E_y field component in zx plot plane in time moments $44\,\Delta t$, $80\,\Delta t$, $156\,\Delta t$, $240\,\Delta t$, $283\,\Delta t$ and $606\,\Delta t$, respectively. Only computational domain is presented, CPML layers are excluded from the view. It can be clearly noticed that that the wave is properly formed and propagating without reflections from the side edges of computational domain.

In time moments presented in Figs.4-5 the propagating wave has come to the end of computational domain. There are no undesirable reflections. In Fig. 6 the propagating wave is totally absorbed by CPML, which simulates the propagation through the free space. Still, there are no un-

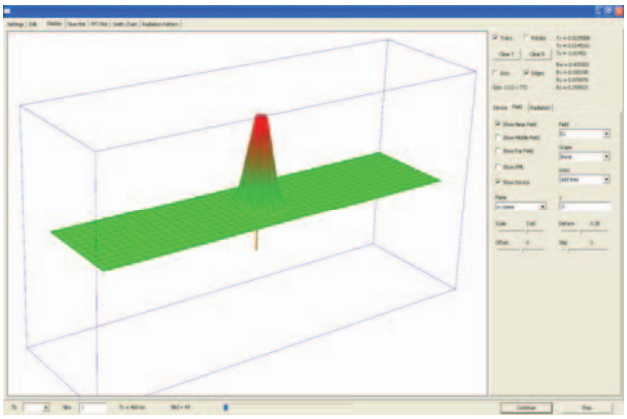

Fig. 1. Propagation of E_y field component in zx plot plane without CPML presented for $t = 44\Delta t$.

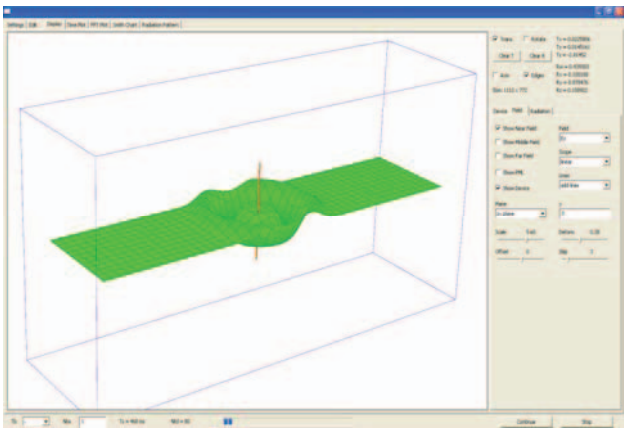

Fig. 2. Propagation of E_y field component in zx plot plane without CPML presented for $t = 80\Delta t$.

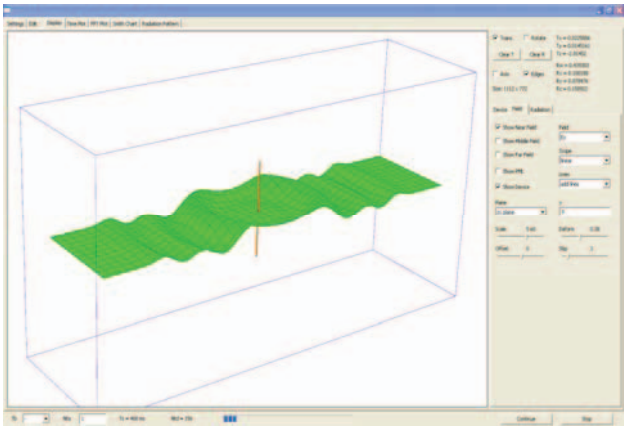

Fig. 3. Propagation of E_y field component in zx plot plane without CPML presented for $t = 156\Delta t$.

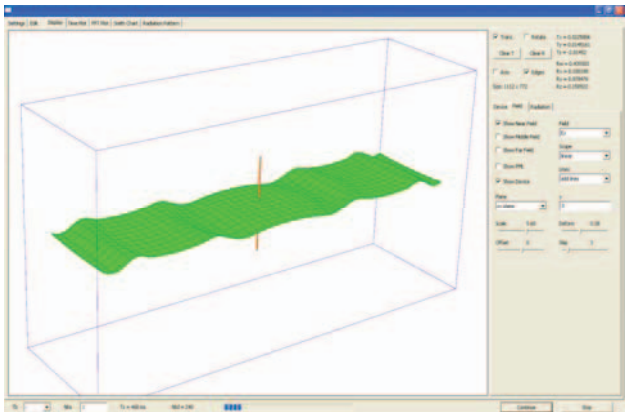

Fig. 4. Propagation of E_y field component in *zx* plot plane without CPML presented for $t = 240\Delta t$.

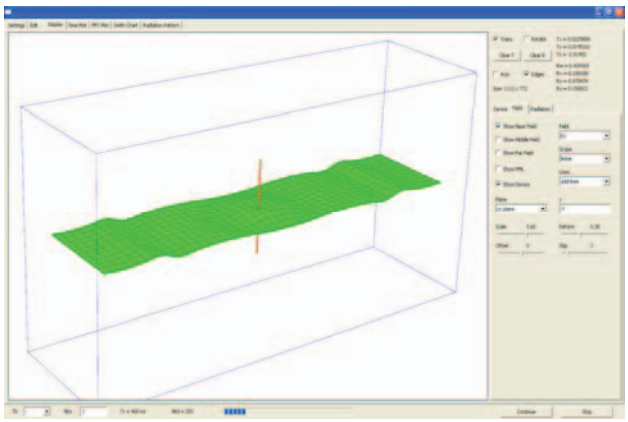

Fig. 5. Propagation of E_y field component in *zx* plot plane without CPML presented for $t = 283\Delta t$.

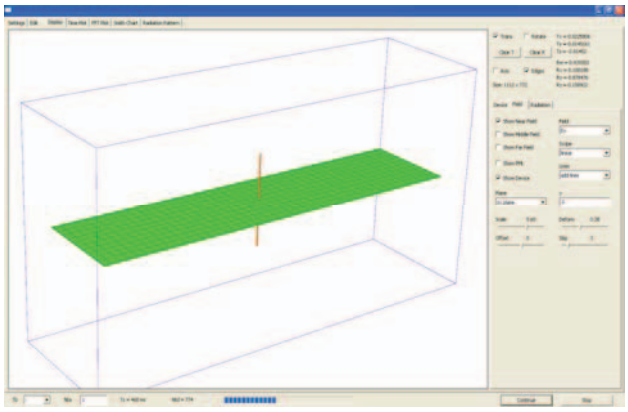

Fig. 6. Propagation of E_y field component in *zx* plot plane without CPML presented for $t = 606\Delta t$.

desirable reflections. This clearly demonstrates the proper functioning of the modified CPML.

In Fig. 7 the propagation of E_y field component in *zx* plot plane is presented in the same time moment as in Fig. 2, but with shown CPML layers. One can observe how the propagating wave at the boundary penetrates into the CPML region. In this region the wave is gradually attenuated and it practically disappears in the vicinity of perfect electric conductor (PEC) wall on the outer side of CPML.

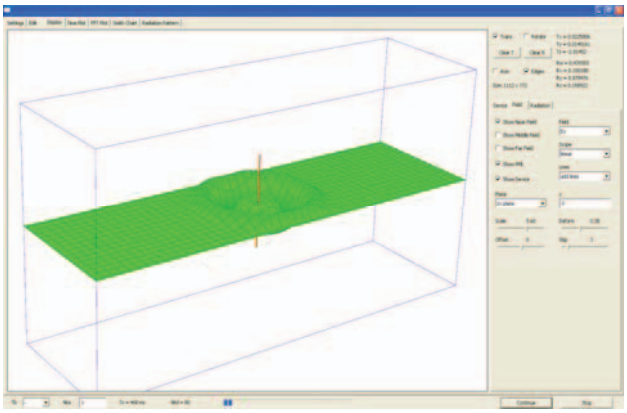

Fig. 7. Propagation of E_y field component in *zx* plot plane with CPML presented for $t = 80\Delta t$.

V. Conclusion

In this paper a modification of conventional CPML is performed in order to support termination of CE-FDTD computational domain. The modified CPML, along with CE-FDTD algorithm has been implemented in an own developed simulation environment.

The functionality of the proposed CPML is tested on various simulation cases and illustrated here on the example of dipole antenna. At the end of computational domain, the propagating wave is totally absorbed by CPML. This behavior fully corresponds to the propagation through the free space. There are no undesirable reflections, which clearly demonstrates the proper functioning of the modified CPML.

Here proposed modification of CPML is basically an extension of the conventional CPML to the complex formulation. For this reason, its properties and performance are equivalent to the ones of the conventional formulation, which are extensively studied and proven in the literature.

Appendix

The procedure of derivation for update equations (10)-(13) is presented in this section.

A narrow band signal at the carrier frequency can be thought of as

$$\left(H_{pv}, E_{pv}\right) = \mathrm{Re}\left\{\left(H_v, E_v\right)\right\}, v = x, y, z \qquad \text{(A1)}$$

where H_v and E_v denote associated complex representations.

In the conventional CPML, a stretched coordinate form is introduced as

$$s_i = k_i + \frac{\sigma_i}{\alpha_i + j\omega\varepsilon_0}, \; i = x, y, z \qquad \text{(A2)}$$

where k_i, σ_i and α_i are CPML parameters. When applied to the *x* component of the electric field in Ampere's law in time domain, for example, it is [14]

$$\varepsilon_x \frac{\partial E_x}{\partial t} = \bar{s}_y * \frac{\partial H_z}{\partial y} - \bar{s}_z * \frac{\partial H_y}{\partial z} \qquad \text{(A3)}$$

where $\bar{s}_i(t)$ is the inverse Laplace transform of the inverse of the stretching parameter $s_i(\omega)^{-1}$. The impulse response of $\bar{s}_i(t)$ has the form [8]

$$\bar{s}_i(t) = \frac{\delta(t)}{k_i} - u(t)\frac{\sigma_i}{\varepsilon_0 k_i^2} e^{-\left(\frac{\sigma_i}{\varepsilon_0 k_i}+\frac{\alpha_i}{\varepsilon_0}\right)t} = \\ = \frac{\delta(t)}{k_i} + \zeta_i(t) \tag{A4}$$

where $\delta(t)$ and $u(t)$ are the impulse and step functions, respectively. After applying (A4), (A3) becomes

$$\varepsilon_x \frac{\partial E_x}{\partial t} = \frac{1}{k_y}\frac{\partial H_z}{\partial y} - \frac{1}{k_z}\frac{\partial H_y}{\partial z} + \\ + \zeta_y(t) * \frac{\partial H_z}{\partial y} - \zeta_z(t) * \frac{\partial H_y}{\partial z} \tag{A5}$$

Using standard FDTD formulation, (A5) can be discretized as

$$\varepsilon_x \frac{E^{n+1}_{x(i+1/2,j,k)} - E^{n}_{x(i+1/2,j,k)}}{\Delta t} = \\ = \frac{H^{n+1/2}_{z(i+1/2,j+1/2,k)} - H^{n+1/2}_{z(i+1/2,j-1/2,k)}}{k_y \Delta y} - \\ - \frac{H^{n+1/2}_{y(i+1/2,j,k+1/2)} - H^{n+1/2}_{y(i+1/2,j,k-1/2)}}{k_z \Delta z} + \\ + \sum_{m=0}^{N-1} Z_{0y}(m) \frac{H^{n-m+1/2}_{z(i+1/2,j+1/2,k)} - H^{n-m+1/2}_{z(i+1/2,j-1/2,k)}}{\Delta y} - \\ - \sum_{m=0}^{N-1} Z_{0z}(m) \frac{H^{n-m+1/2}_{y(i+1/2,j,k+1/2)} - H^{n-m+1/2}_{y(i+1/2,j,k-1/2)}}{\Delta z} \tag{A6}$$

where $Z_{0\nu}(m)$, $\nu = y, z$ is discrete impulse response of $\zeta(t)$. It can be represented as

$$Z_{0\nu}(m) = \int_{m\Delta t}^{(m+1)\Delta t} \zeta_\nu(t) = a_\nu e^{\left(\frac{\sigma_\nu}{k_\nu}+\alpha_\nu\right)\frac{m\Delta t}{\varepsilon_0}} \tag{A7}$$

where

$$a_\nu = \frac{\sigma_\nu\left(e^{-\left(\frac{\sigma_\nu}{k_\nu}+\alpha_\nu\right)\frac{\Delta t}{\varepsilon_0}} - 1\right)}{\sigma_\nu k_\nu + k_\nu^2 \alpha_\nu}, \ \nu = y, z. \tag{A8}$$

Since $Z_{0\nu}(m)$ has a simple exponential form, it is possible to perform the convolutions in (A6) through an auxiliary term in recursive form ψ_ν. Now, (A6) becomes

$$\varepsilon_x \frac{E^{n+1}_{x(i+1/2,j,k)} - E^{n}_{x(i+1/2,j,k)}}{\Delta t} = \\ \frac{H^{n+1/2}_{z(i+1/2,j+1/2,k)} - H^{n+1/2}_{z(i+1/2,j-1/2,k)}}{k_y \Delta y} - \\ - \frac{H^{n+1/2}_{y(i+1/2,j,k+1/2)} - H^{n+1/2}_{y(i+1/2,j,k-1/2)}}{k_z \Delta z} + \\ + \psi^{n+1/2}_{e\,x,y(i+1/2,j,k)} - \psi^{n+1/2}_{e\,x,z(i+1/2,j,k)} \tag{A9}$$

where ψ_ν terms are

$$\psi^{n+1/2}_{e\,x,y(i+1/2,j,k)} = b_y \psi^{n-1/2}_{e\,x,y(i+1/2,j,k)} + \\ + a_y \frac{H^{n+1/2}_{z(i+1/2,j+1/2,k)} - H^{n+1/2}_{z(i+1/2,j-1/2,k)}}{\Delta y} \tag{A10}$$

$$\psi^{n+1/2}_{e\,x,z(i+1/2,j,k)} = b_z \psi^{n+1/2}_{e\,x,z(i+1/2,j,k)} + \\ + a_z \frac{H^{n+1/2}_{y(i+1/2,j,k+1/2)} - H^{n+1/2}_{y(i+1/2,j,k-1/2)}}{\Delta z} \tag{A11}$$

with constant b_ν given as

$$b_\nu = e^{-\left(\frac{\sigma_\nu}{k_\nu}+\alpha_\nu\right)\frac{\Delta t}{\varepsilon_0}}. \tag{A12}$$

However, in CE-FDTD formulation, instead of real field components $(H_{p\nu}, E_{p\nu})$, their complex-envelope representations $(\hat{H}_\nu, \hat{E}_\nu)$ are available. In that case update equation (A9) becomes

$$\varepsilon_x \frac{\hat{E}^{n+1}_{x(i+1/2,j,k)} - \hat{E}^{n}_{x(i+1/2,j,k)}}{\Delta t} = \\ \frac{\hat{H}^{n+1/2}_{z(i+1/2,j+1/2,k)} - \hat{H}^{n+1/2}_{z(i+1/2,j-1/2,k)}}{k_y \Delta y} - \\ - \frac{\hat{H}^{n+1/2}_{y(i+1/2,j,k+1/2)} - \hat{H}^{n+1/2}_{y(i+1/2,j,k-1/2)}}{k_z \Delta z} + \\ + \hat{\psi}^{n+1/2}_{e\,x,y(i+1/2,j,k)} - \hat{\psi}^{n+1/2}_{e\,x,z(i+1/2,j,k)} \tag{A13}$$

where

$$\hat{\psi}^{n+1/2}_{ex,y(i+1/2,j,k)} = \psi^{n+1/2}_{ex,y(i+1/2,j,k)} e^{-j\omega_c\left(n+\frac{1}{2}\right)\Delta t} \tag{A14}$$

$$\hat{\psi}^{n+1/2}_{ex,z(i+1/2,j,k)} = \psi^{n+1/2}_{ex,z(i+1/2,j,k)} e^{-j\omega_c\left(n+\frac{1}{2}\right)\Delta t} \tag{A15}$$

It is possible to apply (A10) and (A11) in (A14) and (A15), respectively, only if the relation that follows from (1) and (A1) is used

$$H_{\nu}^{n+1/2} = \hat{H}_{\nu}^{n+1/2} e^{j\omega_c (n+1/2)\Delta t} . \qquad \text{(A16)}$$

After few very straightforward algebraic manipulations the final update equation for x component of electric field in CPML region in CE-FDTD formulation has the form

$$\begin{aligned} \hat{E}_{x(i+1/2,j,k)}^{n+1} &= \hat{E}_{x(i+1/2,j,k)}^{n} + \\ &\frac{\Delta t}{\varepsilon_x} \frac{\hat{H}_{z(i+1/2,j+1/2,k)}^{n+1/2} - \hat{H}_{z(i+1/2,j-1/2,k)}^{n+1/2}}{k_y \Delta y} - \\ &- \frac{\Delta t}{\varepsilon_x} \frac{\hat{H}_{y(i+1/2,j,k+1/2)}^{n+1/2} - \hat{H}_{y(i+1/2,j,k-1/2)}^{n+1/2}}{k_z \Delta z} + \\ &+ \psi_{e\,x,y(i+1/2,j,k)}^{n+1/2} e^{-j\omega_c (n+1/2)\Delta t} - \\ &- \psi_{e\,x,z(i+1/2,j,k)}^{n+1/2} e^{-j\omega_c (n+1/2)\Delta t} \end{aligned} \qquad \text{(A17)}$$

where it is

$$\begin{aligned} \psi_{ex,y(i+1/2,j,k)}^{n+1/2} &= b_y \psi_{e\,x,y(i+1/2,j,k)}^{n-1/2} + \\ &+ a_y \frac{\hat{H}_{z(i+1/2,j+1/2,k)}^{n+1/2}}{\Delta y} e^{j\omega_c \left(n+\frac{1}{2}\right)\Delta t} - \\ &- a_y \frac{\hat{H}_{z(i+1/2,j-1/2,k)}^{n+1/2}}{\Delta y} e^{j\omega_c \left(n+\frac{1}{2}\right)\Delta t} \end{aligned} \qquad \text{(A18)}$$

$$\begin{aligned} \psi_{ex,z(i+1/2,j,k)}^{n+1/2} &= b_z \psi_{e\,x,z(i+1/2,j,k)}^{n+1/2} + \\ &+ a_z \frac{\hat{H}_{y(i+1/2,j,k+1/2)}^{n+1/2}}{\Delta z} e^{j\omega_c \left(n+\frac{1}{2}\right)\Delta t} - \\ &- a_z \frac{\hat{H}_{y(i+1/2,j,k-1/2)}^{n+1/2}}{\Delta z} e^{j\omega_c \left(n+\frac{1}{2}\right)\Delta t} . \end{aligned} \qquad \text{(A19)}$$

Following the similar procedure, one can obtain update equation for the other five field components in CPML region in CE-FDTD formulation. The form of update equation (11) is somewhat different from (A17) since the undertaken code optimization, described in [13], is included in (11).

ACKNOWLEDGMENT

This work is supported in part by the Ministry of Education, Science and Technological Development of Serbia within the Projects TR-32051 and TR-33008.

REFERENCES

[1] K. S. Yee, "Numerical solution of initial boundary value problems involving Maxwell's equations in isotropic media," *IEEE Trans. on Antennas and Propagation*, vol. AP-14, pp. 302–307, May 1966.

[2] A. Taflove and S. C. Hagness, *Computational Electrodynamics: The Finite-Difference Time-Domain Method*. 3rd ed., Norwood, USA: Artech House, 2005.

[3] K. S. Kunz and R. J. Luebbers, *The Finite Difference Time Domain Method for Electromagnetics*. Boca Raton, FL: CRC Press, 1993.

[4] C. Ma and Z. Chen, "Stability and numerical dispersion analysis of CE-FDTD method," *IEEE Trans. on Antennas and Propagation*, vol. 53, no. 1, pp. 332–338, January 2005.

[5] J. D. Pursel and P. M. Goggans, "A finite-difference time-domain method for solving electromagnetic problems with bandpass-limited source," *IEEE Trans. on Antennas and Propagation*, vol. 47, no. 1, pp. 9–15, January 1999.

[6] J.-P. Berenger, "A perfectly matched layer for the absorption of electromagnetic waves," *Journal of Computational Physics*, vol. 114, pp. 195–200, October 1994.

[7] S. D. Gedney, "The perfectly matched layer absorbing medium," in *Advances in computational electrodynamics: The finite difference time domain*, A. Taflove, 1st ed., Boston: Artech House, 1998, pp. 263–340.

[8] J. A. Roden and S. D. Gedney, "Convolution PML (CPML): An efficient FDTD implementation of the CFS–PML for arbitrary media," *Microwave and Optical Technology Lett.*, vol. 27, no. 5, pp. 334–339, December 2000.

[9] W. C. Chew and W. H. Weedon, "A 3-D perfectly matched medium from modified Maxwell's equation with stretched coordinates," *Microwave and Optical Technology Lett.*, vol. 7, pp. 599–604, September 1994.

[10] M. Kuzuoglu and R. Mittra, "Frequency dependence of the constitutive parameters of causal perfectly matched anisotropic absorbers," *IEEE Microw. Guid. Wave Lett.*, vol. 6, pp. 447–449, December 1996.

[11] D. Vidacic, "Assessment of FDTD model parameters for lossy media," Master thesis, University of New Hampshire, September 2003.

[12] D. Y. Heh and E. L. Tan, "Dispersion analysis of FDTD schemes for doubly lossy media," *Progress In Electromagnetics Research B*, vol. 17, pp. 327–342, 2009.

[13] B. Nikolic, B. Dimitrijevic, N. Raicevic, and S. Aleksic, "Implementation of FDTD based simulation environment," *Facta Univ. Ser.: Elec. Energ.*, vol. 26, no. 2, pp. 121–132, August 2013.

[14] U. S. Inan and R. A. Marshall, *Numerical Electromagnetics.* Cambridge, UK: Cambridge University Press, 2011.